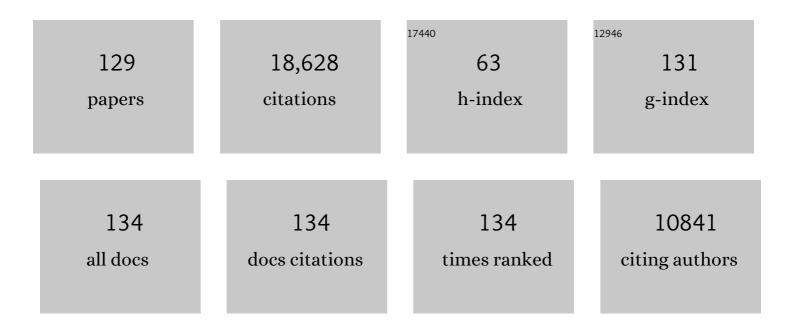
Anton Barty

List of Publications by Year in descending order

Source: https://exaly.com/author-pdf/9455911/publications.pdf Version: 2024-02-01



Δητών Βάρτν

#	Article	IF	CITATIONS
1	Femtosecond X-ray Fourier holography imaging of free-flying nanoparticles. Nature Photonics, 2018, 12, 150-153.	31.4	58
2	Supersaturation-controlled microcrystallization and visualization analysis for serial femtosecond crystallography. Scientific Reports, 2018, 8, 2541.	3.3	4
3	Femtosecond X-ray diffraction from an aerosolized beam of protein nanocrystals. Journal of Applied Crystallography, 2018, 51, 133-139.	4.5	18
4	Ultrafast nonthermal heating of water initiated by an X-ray Free-Electron Laser. Proceedings of the National Academy of Sciences of the United States of America, 2018, 115, 5652-5657.	7.1	28
5	Femtosecond X-ray coherent diffraction of aligned amyloid fibrils on low background graphene. Nature Communications, 2018, 9, 1836.	12.8	34
6	Resolution extension by image summing in serial femtosecond crystallography of two-dimensional membrane-protein crystals. IUCrJ, 2018, 5, 103-117.	2.2	8
7	Structural enzymology using X-ray free electron lasers. Structural Dynamics, 2017, 4, 044003.	2.3	92
8	Atomic structure of granulin determined from native nanocrystalline granulovirus using an X-ray free-electron laser. Proceedings of the National Academy of Sciences of the United States of America, 2017, 114, 2247-2252.	7.1	65
9	Diffraction data of core-shell nanoparticles from an X-ray free electron laser. Scientific Data, 2017, 4, 170048.	5.3	4
10	Flowâ€aligned, singleâ€shot fiber diffraction using a femtosecond Xâ€ray freeâ€electron laser. Cytoskeleton, 2017, 74, 472-481.	2.0	12
11	Double-flow focused liquid injector for efficient serial femtosecond crystallography. Scientific Reports, 2017, 7, 44628.	3.3	90
12	Identification of Phosphorylation Codes for Arrestin Recruitment by G Protein-Coupled Receptors. Cell, 2017, 170, 457-469.e13.	28.9	344
13	From Macrocrystals to Microcrystals: A Strategy for Membrane Protein Serial Crystallography. Structure, 2017, 25, 1461-1468.e2.	3.3	21
14	Coherent soft X-ray diffraction imaging of coliphage PR772 at the Linac coherent light source. Scientific Data, 2017, 4, 170079.	5.3	54
15	Structures of riboswitch RNA reaction states by mix-and-inject XFEL serial crystallography. Nature, 2017, 541, 242-246.	27.8	251
16	Post-sample aperture for low background diffraction experiments at X-ray free-electron lasers. Journal of Synchrotron Radiation, 2017, 24, 1296-1298.	2.4	8
17	Continuous diffraction of molecules and disordered molecular crystals. Journal of Applied Crystallography, 2017, 50, 1084-1103.	4.5	21
18	Experimental strategies for imaging bioparticles with femtosecond hard X-ray pulses. IUCrJ, 2017, 4, 251-262.	2.2	63

#	Article	IF	CITATIONS
19	Analysis of XFEL serial diffraction data from individual crystalline fibrils. IUCrJ, 2017, 4, 795-811.	2.2	16
20	Open data set of live cyanobacterial cells imaged using an X-ray laser. Scientific Data, 2016, 3, 160058.	5.3	7
21	<i>OnDA</i> : online data analysis and feedback for serial X-ray imaging. Journal of Applied Crystallography, 2016, 49, 1073-1080.	4.5	89
22	A data set from flash X-ray imaging of carboxysomes. Scientific Data, 2016, 3, 160061.	5.3	11
23	Single molecule imaging using X-ray free electron lasers. Current Opinion in Structural Biology, 2016, 40, 186-194.	5.7	14
24	Coherent diffraction of single Rice Dwarf virus particles using hard X-rays at the Linac Coherent Light Source. Scientific Data, 2016, 3, 160064.	5.3	64
25	Lipidic cubic phase injector is a viable crystal delivery system for time-resolved serial crystallography. Nature Communications, 2016, 7, 12314.	12.8	71
26	Single-shot diffraction data from the Mimivirus particle using an X-ray free-electron laser. Scientific Data, 2016, 3, 160060.	5.3	18
27	Femtosecond structural dynamics drives the trans/cis isomerization in photoactive yellow protein. Science, 2016, 352, 725-729.	12.6	348
28	Native phasing of x-ray free-electron laser data for a G protein–coupled receptor. Science Advances, 2016, 2, e1600292.	10.3	97
29	The room temperature crystal structure of a bacterial phytochrome determined by serial femtosecond crystallography. Scientific Reports, 2016, 6, 35279.	3.3	39
30	X-ray laser diffraction for structure determination of the rhodopsin-arrestin complex. Scientific Data, 2016, 3, 160021.	5.3	51
31	Serial femtosecond crystallography datasets from G protein-coupled receptors. Scientific Data, 2016, 3, 160057.	5.3	10
32	Macromolecular diffractive imaging using imperfect crystals. Nature, 2016, 530, 202-206.	27.8	123
33	Recent developments in <i>CrystFEL</i> . Journal of Applied Crystallography, 2016, 49, 680-689.	4.5	222
34	Direct Phasing of Finite Crystals Illuminated with a Free-Electron Laser. Physical Review X, 2015, 5, .	8.9	12
35	Electronic damage in S atoms in a native protein crystal induced by an intense X-ray free-electron laser pulse. Structural Dynamics, 2015, 2, 041703.	2.3	20
36	Towards phasing using high X-ray intensity. IUCrJ, 2015, 2, 627-634.	2.2	24

#	Article	IF	CITATIONS
37	Serial femtosecond crystallography of soluble proteins in lipidic cubic phase. IUCrJ, 2015, 2, 545-551.	2.2	61
38	The linac coherent light source single particle imaging road map. Structural Dynamics, 2015, 2, 041701.	2.3	178
39	Strongly aligned gas-phase molecules at free-electron lasers. Journal of Physics B: Atomic, Molecular and Optical Physics, 2015, 48, 204002.	1.5	28
40	Accurate determination of segmented X-ray detector geometry. Optics Express, 2015, 23, 28459.	3.4	69
41	Trace phase detection and strain characterization from serial X-ray free-electron laser crystallography of a Pr _{0.5} Ca _{0.5} MnO ₃ powder. Powder Diffraction, 2015, 30, S25-S30.	0.2	1
42	Ternary structure reveals mechanism of a membrane diacylglycerol kinase. Nature Communications, 2015, 6, 10140.	12.8	30
43	Imaging single cells in a beam of live cyanobacteria with an X-ray laser. Nature Communications, 2015, 6, 5704.	12.8	156
44	Structural basis for bifunctional peptide recognition at human δ-opioid receptor. Nature Structural and Molecular Biology, 2015, 22, 265-268.	8.2	151
45	Three-Dimensional Reconstruction of the Giant Mimivirus Particle with an X-Ray Free-Electron Laser. Physical Review Letters, 2015, 114, 098102.	7.8	284
46	Indications of radiation damage in ferredoxin microcrystals using high-intensity X-FEL beams. Journal of Synchrotron Radiation, 2015, 22, 225-238.	2.4	110
47	Effects of self-seeding and crystal post-selection on the quality of Monte Carlo-integrated SFX data. Journal of Synchrotron Radiation, 2015, 22, 644-652.	2.4	20
48	Anomalous Behavior of the Homogeneous Ice Nucleation Rate in "No-Man's Land― Journal of Physical Chemistry Letters, 2015, 6, 2826-2832.	4.6	102
49	Crystal structure of rhodopsin bound to arrestin by femtosecond X-ray laser. Nature, 2015, 523, 561-567.	27.8	683
50	High numerical aperture multilayer Laue lenses. Scientific Reports, 2015, 5, 9892.	3.3	89
51	Ultrafast self-gating Bragg diffraction of exploding nanocrystals in an X-ray laser. Optics Express, 2015, 23, 1213.	3.4	29
52	<i>Cheetah</i> : software for high-throughput reduction and analysis of serial femtosecond X-ray diffraction data. Journal of Applied Crystallography, 2014, 47, 1118-1131.	4.5	348
53	Toward atomic resolution diffractive imaging of isolated molecules with X-ray free-electron lasers. Faraday Discussions, 2014, 171, 393-418.	3.2	29
54	Automated identification and classification of single particle serial femtosecond X-ray diffraction data. Optics Express, 2014, 22, 2497.	3.4	45

#	Article	IF	CITATIONS
55	Explosion dynamics of sucrose nanospheres monitored by time of flight spectrometry and coherent diffractive imaging at the split-and-delay beam line of the FLASH soft X-ray laser. Optics Express, 2014, 22, 28914.	3.4	13
56	Time-resolved serial crystallography captures high-resolution intermediates of photoactive yellow protein. Science, 2014, 346, 1242-1246.	12.6	418
57	Phasing coherently illuminated nanocrystals bounded by partial unit cells. Philosophical Transactions of the Royal Society B: Biological Sciences, 2014, 369, 20130331.	4.0	29
58	Mapping the continuous reciprocal space intensity distribution of X-ray serial crystallography. Philosophical Transactions of the Royal Society B: Biological Sciences, 2014, 369, 20130333.	4.0	29
59	Lipidic cubic phase injector facilitates membrane protein serial femtosecond crystallography. Nature Communications, 2014, 5, 3309.	12.8	505
60	High-throughput imaging of heterogeneous cell organelles with an X-ray laser. Nature Photonics, 2014, 8, 943-949.	31.4	156
61	7 Ã resolution in protein two-dimensional-crystal X-ray diffraction at Linac Coherent Light Source. Philosophical Transactions of the Royal Society B: Biological Sciences, 2014, 369, 20130500.	4.0	32
62	Visualizing a protein quake with time-resolved X-ray scattering at a free-electron laser. Nature Methods, 2014, 11, 923-926.	19.0	173
63	Ultrafast X-ray probing of water structure below the homogeneous ice nucleation temperature. Nature, 2014, 510, 381-384.	27.8	385
64	Serial time-resolved crystallography of photosystem II using a femtosecond X-ray laser. Nature, 2014, 513, 261-265.	27.8	403
65	Room-temperature macromolecular serial crystallography using synchrotron radiation. IUCrJ, 2014, 1, 204-212.	2.2	221
66	X-Ray Diffraction from Isolated and Strongly Aligned Gas-Phase Molecules with a Free-Electron Laser. Physical Review Letters, 2014, 112, .	7.8	217
67	Fixed-target protein serial microcrystallography with an x-ray free electron laser. Scientific Reports, 2014, 4, 6026.	3.3	169
68	Serial Femtosecond Crystallography of G Protein–Coupled Receptors. Science, 2013, 342, 1521-1524.	12.6	424
69	Structure of a photosynthetic reaction centre determined by serial femtosecond crystallography. Nature Communications, 2013, 4, 2911.	12.8	74
70	Natively Inhibited <i>Trypanosoma brucei</i> Cathepsin B Structure Determined by Using an X-ray Laser. Science, 2013, 339, 227-230.	12.6	393
71	Molecular Imaging Using X-Ray Free-Electron Lasers. Annual Review of Physical Chemistry, 2013, 64, 415-435.	10.8	156
72	Crystallographic data processing for free-electron laser sources. Acta Crystallographica Section D: Biological Crystallography, 2013, 69, 1231-1240.	2.5	122

#	Article	IF	CITATIONS
73	Sensing the wavefront of x-ray free-electron lasers using aerosol spheres. Optics Express, 2013, 21, 12385.	3.4	28
74	Toward unsupervised single-shot diffractive imaging of heterogeneous particles using X-ray free-electron lasers. Optics Express, 2013, 21, 28729.	3.4	20
75	Mesoscale morphology of airborne core–shell nanoparticle clusters: x-ray laser coherent diffraction imaging. Journal of Physics B: Atomic, Molecular and Optical Physics, 2013, 46, 164033.	1.5	12
76	Femtosecond free-electron laser x-ray diffraction data sets for algorithm development. Optics Express, 2012, 20, 4149.	3.4	56
77	Noise-robust coherent diffractive imaging with a single diffraction pattern. Optics Express, 2012, 20, 16650.	3.4	73
78	Time-resolved protein nanocrystallography using an X-ray free-electron laser. Optics Express, 2012, 20, 2706.	3.4	219
79	Femtosecond dark-field imaging with an X-ray free electron laser. Optics Express, 2012, 20, 13501.	3.4	38
80	CASS—CFEL-ASG software suite. Computer Physics Communications, 2012, 183, 2207-2213.	7.5	65
81	Lipidic phase membrane protein serial femtosecond crystallography. Nature Methods, 2012, 9, 263-265.	19.0	135
82	Fractal morphology, imaging and mass spectrometry of single aerosol particles in flight. Nature, 2012, 486, 513-517.	27.8	170
83	New Avenues for Structure Determination of Membrane Proteins. Biophysical Journal, 2012, 102, 3a.	0.5	0
84	Self-terminating diffraction gates femtosecond X-ray nanocrystallography measurements. Nature Photonics, 2012, 6, 35-40.	31.4	292
85	Single-particle structure determination by correlations of snapshot X-ray diffraction patterns. Nature Communications, 2012, 3, 1276.	12.8	76
86	In vivo protein crystallization opens new routes in structural biology. Nature Methods, 2012, 9, 259-262.	19.0	193
87	High-Resolution Protein Structure Determination by Serial Femtosecond Crystallography. Science, 2012, 337, 362-364.	12.6	758
88	<i>CrystFEL</i> : a software suite for snapshot serial crystallography. Journal of Applied Crystallography, 2012, 45, 335-341.	4.5	410
89	Phasing of coherent femtosecond X-ray diffraction from size-varying nanocrystals. Optics Express, 2011, 19, 2866.	3.4	82
90	Unsupervised classification of single-particle X-ray diffraction snapshots by spectral clustering. Optics Express, 2011, 19, 16542.	3.4	91

#	Article	IF	CITATIONS
91	Radiation damage in protein serial femtosecond crystallography using an x-ray free-electron laser. Physical Review B, 2011, 84, 214111.	3.2	156
92	Single mimivirus particles intercepted and imaged with an X-ray laser. Nature, 2011, 470, 78-81.	27.8	790
93	Femtosecond X-ray protein nanocrystallography. Nature, 2011, 470, 73-77.	27.8	1,771
94	Structure-factor analysis of femtosecond microdiffraction patterns from protein nanocrystals. Acta Crystallographica Section A: Foundations and Advances, 2011, 67, 131-140.	0.3	128
95	Multipurpose modular experimental station for the DiProl beamline of Fermi@Elettra free electron laser. Review of Scientific Instruments, 2011, 82, 043711.	1.3	28
96	Single-shot femtosecond x-ray diffraction from randomly oriented ellipsoidal nanoparticles. Physical Review Special Topics: Accelerators and Beams, 2010, 13, .	1.8	13
97	Aerosol Imaging with a Soft X-Ray Free Electron Laser. Aerosol Science and Technology, 2010, 44, i-vi.	3.1	40
98	Femtosecond diffractive imaging of biological cells. Journal of Physics B: Atomic, Molecular and Optical Physics, 2010, 43, 194015.	1.5	41
99	Time-resolved imaging using x-ray free electron lasers. Journal of Physics B: Atomic, Molecular and Optical Physics, 2010, 43, 194014.	1.5	16
100	Publisher's Note: Cryptotomography: Reconstructing 3D Fourier Intensities from Randomly Oriented Single-Shot Diffraction Patterns [Phys. Rev. Lett.104, 225501 (2010)]. Physical Review Letters, 2010, 104, .	7.8	6
101	Cryptotomography: Reconstructing 3D Fourier Intensities from Randomly Oriented Single-Shot Diffraction Patterns. Physical Review Letters, 2010, 104, 225501.	7.8	94
102	Sacrificial Tamper Slows Down Sample Explosion in FLASH Diffraction Experiments. Physical Review Letters, 2010, 104, 064801.	7.8	59
103	Predicting the coherent X-ray wavefront focal properties at the Linac Coherent Light Source (LCLS) X-ray free electron laser. Optics Express, 2009, 17, 15508.	3.4	62
104	Ultrafast soft X-ray scattering and reference-enhanced diffractive imaging of weakly scattering nanoparticles. Journal of Electron Spectroscopy and Related Phenomena, 2008, 166-167, 65-73.	1.7	16
105	Ultrafast single-shot diffraction imaging of nanoscale dynamics. Nature Photonics, 2008, 2, 415-419.	31.4	221
106	Massively parallel X-ray holography. Nature Photonics, 2008, 2, 560-563.	31.4	168
107	Single Particle X-ray Diffractive Imaging. Nano Letters, 2008, 8, 310-316.	9.1	229
108	Camera for coherent diffractive imaging and holography with a soft-x-ray free-electron laser. Applied Optics, 2008, 47, 1673.	2.1	34

#	Article	IF	CITATIONS
109	Three-Dimensional Coherent X-Ray Diffraction Imaging of a Ceramic Nanofoam: Determination of Structural Deformation Mechanisms. Physical Review Letters, 2008, 101, 055501.	7.8	106
110	Validation of radiographic simulation codes including x-ray phase effects for millimeter-size objects with micrometer structures. Journal of the Optical Society of America A: Optics and Image Science, and Vision, 2007, 24, 169.	1.5	8
111	Femtosecond time-delay X-ray holography. Nature, 2007, 448, 676-679.	27.8	238
112	High-resolution ab initio three-dimensional x-ray diffraction microscopy. Journal of the Optical Society of America A: Optics and Image Science, and Vision, 2006, 23, 1179.	1.5	511
113	Femtosecond diffractive imaging with a soft-X-ray free-electron laser. Nature Physics, 2006, 2, 839-843.	16.7	910
114	Actinic inspection of extreme ultraviolet programed multilayer defects and cross-comparison measurements. Journal of Vacuum Science & Technology B, 2006, 24, 2824.	1.3	28
115	Quantitative characterization of inertial confinement fusion capsules using phase contrast enhanced x-ray imaging. Journal of Applied Physics, 2005, 97, 063103.	2.5	56
116	X-ray imaging of cryogenic deuterium-tritium layers in a beryllium shell. Journal of Applied Physics, 2005, 98, 103105.	2.5	37
117	Damped and thermal motion of laser-aligned hydrated macromolecule beams for diffraction. Journal of Chemical Physics, 2005, 123, 244304.	3.0	20
118	Repair of phase defects in extreme-ultraviolet lithography mask blanks. Journal of Applied Physics, 2004, 96, 6812-6821.	2.5	9
119	Quantitative phase-amplitude microscopy. III. The effects of noise. Journal of Microscopy, 2004, 214, 51-61.	1.8	182
120	Repairing amplitude defects in multilayer-coated extreme-ultraviolet lithography reticles by use of a focused ion beam. Applied Optics, 2004, 43, 6545.	2.1	3
121	Testing extreme ultraviolet optics with visible-light and extreme ultraviolet interferometry. Journal of Vacuum Science & Technology an Official Journal of the American Vacuum Society B, Microelectronics Processing and Phenomena, 2002, 20, 2834.	1.6	17
122	Refractive-index profiling of optical fibers with axial symmetry by use of quantitative phase microscopy. Optics Letters, 2002, 27, 2061.	3.3	89
123	Quantitative phase-amplitude microscopy I: optical microscopy. Journal of Microscopy, 2002, 206, 194-203.	1.8	181
124	The holographic twin image problem: a deterministic phase solution. Optics Communications, 2000, 183, 7-14.	2.1	22
125	Quantitative phase tomography. Optics Communications, 2000, 175, 329-336.	2.1	133
126	Quantitative phase-sensitive imaging in a transmission electron microscope. Ultramicroscopy, 2000, 83, 67-73.	1.9	180

#	Article	IF	CITATIONS
127	Noninterferometric quantitative phase imaging with soft x rays. Journal of the Optical Society of America A: Optics and Image Science, and Vision, 2000, 17, 1732.	1.5	43
128	Sub-wavelength characterisation of optical focal structures. Optics Communications, 1998, 145, 9-14.	2.1	14
129	Quantitative optical phase microscopy. Optics Letters, 1998, 23, 817.	3.3	500